

## Experimental Study on the Creep Behavior of Recombinant Bamboo

Yang Wei\*, Kunpeng Zhao, Chen Hang, Si Chen and Mingmin Ding

College of Civil Engineering, Nanjing Forestry University, Nanjing, 210037, China

\*Corresponding Author: Yang Wei. Email: wy78@njfu.edu.cn

Received: 08 October 2019; Accepted: 06 January 2020

**Abstract:** The creep behavior of bamboo due to the complicated influences of environment and stress will lead to a sustained increase in deformation, which serious effects the service performance of structures. To investigate the creep behavior of recombinant bamboo, twenty-four recombinant bamboo specimens were tested under lasting compressive and tensile loads at different load levels. The typical failure modes of recombinant bamboo under a lasting load at a high load level were buckling failure and brittle fracturing due to creep compressive creep and tensile creep development, respectively. At a high load level, the creep deformation of recombinant bamboo initially develops unsteadily and increases rapidly until failure; at a low load level, creep deformation rapidly develops in the early stage and stabilizes in the middle and late stages. The load level has notable effects on the overall creep deformation and the proportion of creep deformation. The residual deformation of creep will generally increase and the recovery of creep will decrease with increasing load level. Based on the Burgers model, predictive models that can take the load levels into account were proposed to evaluate the compressive and tensile creep behaviors of recombinant bamboo. The proposed models can be used to accurately evaluate the strain-time behavior of recombinant bamboo.

**Keywords:** Bamboo; creep; load level; Burgers model; creep behavior; predictive model

### 1 Introduction

Due to the high energy consumption, cracking and corrosion of traditional concrete and steel materials, researchers have been trying to develop new structural materials [1-5]. Bamboo, characterized by a low carbon content, sustainable regeneration and excellent mechanical properties [6-12], has been increasingly studied as a building material [13-20]. Researchers have noted the mechanical properties and applications of bamboo materials [21-24]. The experimental study of the bending performance of bamboo by Obataya et al. shows that the bending resistance capacity of bamboo is mainly determined by the combination of the fiber-rich outer layer and the compressible inner layer [25]. Jain et al. tested the mechanical properties of bamboo fiber composites and found that bamboo fiber composites exhibited near-linear elastic behavior [26]. In addition, earlier studies found that the mechanical properties of bamboo are influenced by many factors [27]. Cui et al. examined the relationship between the average number of vascular



This work is licensed under a Creative Commons Attribution 4.0 International License, which permits unrestricted use, distribution, and reproduction in any medium, provided the original work is properly cited.

bundles and the compressive strength of *Phyllostachys pubescens* and *Phyllostachys* tall bamboo [28]. Chung et al. tested the compression and bending properties of two kinds of bamboo, *Bambusa pervariabilis* and *Phyllostachys pubescens*, and determined the characteristic values of the strength and Young's modulus of bamboo species based on the limit state design method [14]. Zou et al. demonstrated the effects of the moisture content on the bending strength, bending pattern and rigidity of bamboo and showed that the bending strength and extent of bamboo materials decreased significantly with increasing moisture content [29]. Kumar et al. studied the effects of bamboo density on its mechanical properties and investigated the stretching, compression, shearing and bending properties of three test pieces with different densities [30]. Das et al. treated bamboo strips with alkaline solutions to study the tensile strength and elastic modulus of the strips [31]. Hu et al. investigated the effects of the strain rate on the compression performance of bamboo and illustrated the damage pattern and failure mechanism of bamboo through photographs of the final deformation of the bamboo microstructure [32]. Adopting steam blasting technology to extract bamboo fibers from raw bamboo, Okubo et al. compared the mechanical properties of that material with the mechanical properties of bamboo composite materials through mechanically extracted fibers and revealed that the tensile strength and modulus of the polypropylene-based composite materials extracted by steam blasting were 15% and 30% greater, respectively [33]. The above discussion suggests that the basic mechanical properties of bamboo materials have been thoroughly investigated.

Bamboo has mechanical properties similar to those of wood and thus can be regarded as an anisotropic viscoelastic material [28,29,34-36]. Due to the complicated influences of environment and stress, bamboo is likely to exhibit creep phenomena similar to those of wood. Creep phenomena will lead to the deformation of the structural component exceeding the limit and cause potential security issues. To evaluate the long-term performance of bamboo structures [37,38], it is important to study the creep characteristics and predictive models of recombinant bamboo. The creep behavior of wood has been well studied [39-41]; some scholars studied the effects of temperature and humidity on the creep properties of wood [42-45]. Tamrakar et al. applied the principle of time-temperature equivalence to simulate the long-term creep properties of wood [46]. Reichel et al. considered the influence of environmental humidity and established a mathematical model under the coupling effect of humidity and mechanical force [47]. Ozyhar et al. conducted creep tests of beech wood in all directions of tension and compression and revealed the viscoelastic character of wood has a significant influence on the mechanical behavior [48]. Wang et al. provided an in-depth discussion on the important factors (load level) affecting wood creep [49]. For bamboo creep, a small number of studies have been conducted. Gottron et al. conducted bamboo creep tests, which showed that the fabric direction of the specimens had a significant effect on the creep behavior and residual strength [50]. Xu et al. used a modified Burgers model to fit creep data of bamboo-based fiber composites and showed that the fully stretched Burgers model can better predict the tensile creep behavior of bamboo-based fiber composites [51]. Kanzaw et al. revealed the influence of fiber content on microscopic creep [52]. However, quantitative creep models of bamboo under tensile and compressive loads have not been systematically studied and established. Bamboo can be manufactured into a number of various products, such as laminated bamboo lumber and recombinant bamboo. In these modern bamboo products, recombinant bamboo has especially favorable mechanical properties and is suitable for structural components. Therefore, recombinant bamboo was used in this test to investigate the creep behavior of bamboo components. Twenty-four short-term creep test specimens are designed and tested in this paper, and tests of tensile and compressive creep are carried out according to relevant specifications. By carefully analyzing bamboo viscous elasticity mechanics, the Burgers model is used to describe the creep characteristics of bamboo, and the relevant viscous elasticity parameters were presented based on the test results, while complete creep models were established for recombinant bamboo under tensile and compressive loadings.

## 2 Materials and Methods

### 2.1 Materials

The recombinant bamboo specimens used in this test were made of parallel-to-grain bamboo-based materials using a hot-pressing adhesive. The processing technology is shown in Fig. 1. There are five main steps in the production of recombinant bamboo: the bamboo is split vertically, bamboo wax is removed, bamboo fibers are rolled into bamboo fiber bundles, bamboo fibers are soaked in glue, and finally, bamboo fibers are adhered by hot pressing. The specifics of this process are described in detail in the literature [53]. The density of the specimens is  $1.23 \text{ g/cm}^3$ , the water content is 8.4%, and the internal glue strength is 3.57 MPa. The material characteristic parameters of recombinant bamboo at normal temperatures were obtained by the mechanical property test: the average compressive strength was 72.25 MPa, and the corresponding variation coefficient was 17.50%; the average tensile strength was 98.48 MPa, and the corresponding variation coefficient was 21.35%. Additionally, the short-term creep load level was determined according to the average of the limit load.

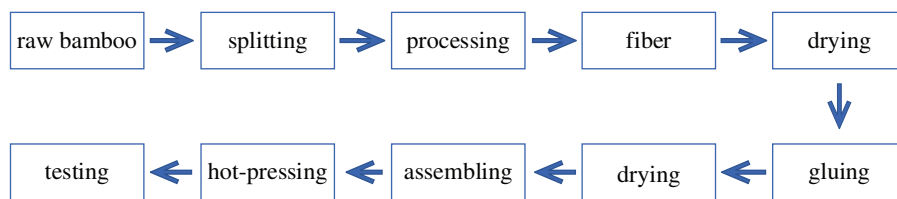


**Figure 1:** Recombinant bamboo production process

The short-term creep tests of recombinant bamboo were carried out in the Nanjing Forestry University Structural Engineering Laboratory. The dimensions of the specimens are determined by referencing the U.S. specification of ASTM D143-94 (2000), “Standard Test Methods for Small Clear Specimens of Timber 1” [54], and China’s national standard GB/T1928-2009, “General Requirements for Physical and Mechanical Tests of Wood” [55]. The dimensions of the compressive specimens were 120 mm (L) × 25 mm (W) × 25 mm (H). For the tensile specimens, the dimensions were 420 mm (L) × 25 mm (W) × 10 mm (H), and the length of the middle part of the tensile specimens was 63 mm with a width and height of 10 mm, while the transition segments had a 444 circular curve radius. Diagrams of the samples are shown in Fig. 2.

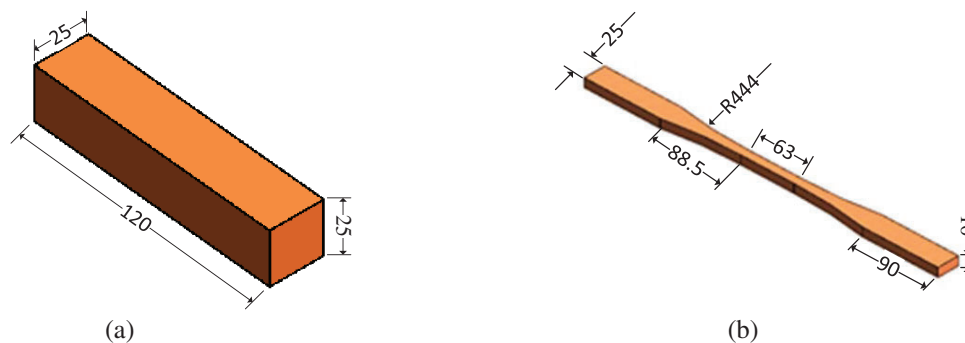


**Figure 2:** Sample diagram of the recombinant bamboo specimens. (a) Compressive specimen (mm). (b) Tensile specimen (mm)

## 2.2 Creep Experiment

The short-term compressive and tensile creep behaviors of recombinant bamboo were tested according to Chinese standard GB1935-2009, “Method of testing in compressive strength parallel to grain of wood” [56], and Chinese standard GB1938-2009, “Method of testing in tensile strength parallel to grain of wood” [57], respectively.

The creep test instrument was a computer-controlled electronic creep long-term test machine (UTM5504-GD) with a maximum test force of 50 kN and an environmental testing chamber (WGDY-7350L) with temperatures ranging from  $-70^{\circ}\text{C}$  to  $350^{\circ}\text{C}$  and humidity from 20% to 100%. This instrument can be used for creep testing of materials, and according to the test results, the strength, deformation, fracture elongation and other relevant creep parameters can be obtained. At the same time, the corresponding stress-strain and creep test curves can be calculated.

A temperature of  $40^{\circ}\text{C}$  and a humidity of 60% were employed for the creep tests in this study. All the creep specimens were polished, resulting in smooth surfaces. Before the short-term creep test, to ensure the internal temperature and humidity balance, the specimens were placed in a chamber with a constant temperature of  $40^{\circ}\text{C}$  and a constant humidity of 60% for more than 6 hours. After the preheat treatment, an extensometer was placed along a 50 mm length in the middle parts of the specimens to determine the deformation-time relationship of the reconstituted bamboo. The extensometer positions of the recombinant bamboo are shown in Fig. 3.

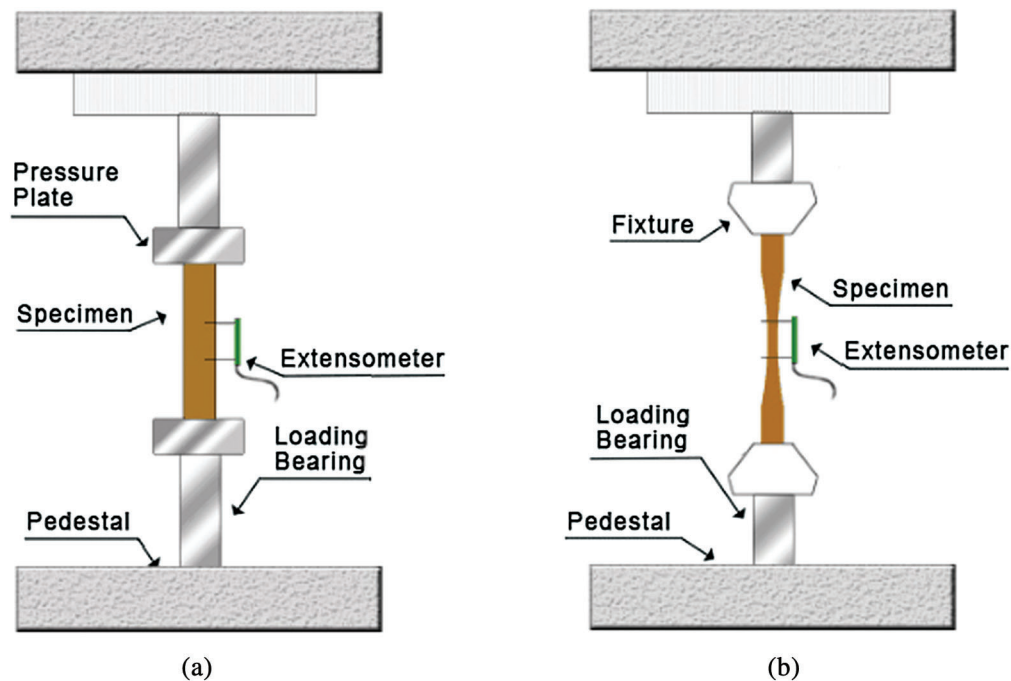


**Figure 3:** Test diagrams of the short-term creep tests of the recombinant bamboo. (a) Compressive creep. (b) Tensile creep

## 2.3 Experimental Program

The test schemes are listed in Tab. 1. There were two types of tests performed: compressive creep and tensile creep tests. The tests comprised eight groups, with a total of twenty-four specimens. In the specimen number, the two digits after “C-” are the load level (%), and “01-03” represents the specimen number. In this

**Table 1:** Short-term creep test schemes for the recombinant bamboo

Test type	Groups	Specimens	Ultimate stress (MPa)	Loading level (%)	Stress (MPa)	Test time (hours)	Number of specimens
Compressive creep	C-10	C-1001-03	72.25	10	7.30	6	3
	C-20	C-2001-03		20	14.50	6	3
	C-40	C-4001-03		40	28.90	6	3
	C-60	C-6001-03		60	43.40	6	3
Tensile creep	T-10	T-1001-03	98.48	10	9.84	6	3
	T-20	T-2001-03		20	19.69	6	3
	T-40	T-4001-03		40	39.39	6	3
	T-60	T-6001-03		60	59.08	6	3

work, the average compressive and tensile strength values of the materials were measured. According to the ultimate strength (72.25 MPa and 98.48 MPa, respectively) and loading level (10%, 20%, 40%, and 60%), the stress values are calculated. Then, the creep tests were carried out for 6 hours.

### 3 Test Results

#### 3.1 Creep Phenomenon

For the four groups of recombinant bamboo compressive creep specimens, when the short-term applied compressive stress is lower than the 40% strength level, no distinct signs of macroscopic failure were observed on the surfaces of the specimens after 6 hours of compressive creep testing, as shown in Fig. 4. When the short-term compressive stress reaches the 60% strength level, with the increase in loading time, a significant failure phenomenon was observed on the surface of the specimens, as shown in Fig. 5. Due to the high stress level, the C-6001 and C-6002 specimens were subjected to buckling failure 30 minutes into the test, and the C-6003 specimen was subjected to buckling failure at the 4.53 hours into the test. In the C-6001 specimen, macroscopic cracks were observed in the longitudinal direction of the upper part, and the upper part of the specimen showed a tendency to protrude outward, while bamboo fibers around the crack were extruded (Fig. 5(a)). For the C-6002 specimen, vertical macroscopic cracks extended

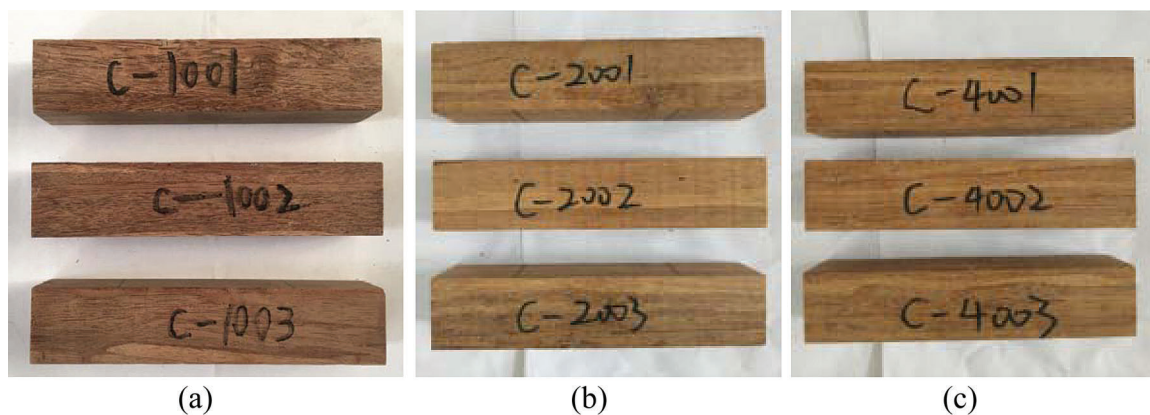


**Figure 4:** Appearance of the bamboo compressive creep specimens at low load levels. (a) Group C-10. (b) Group C-20. (c) Group C-40

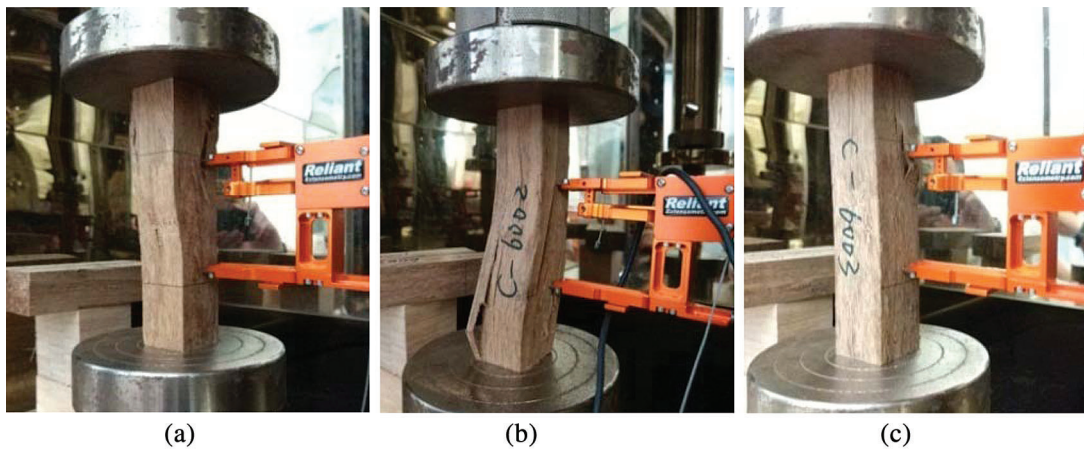


**Figure 5:** Failure phenomena of the bamboo compressive creep specimens at high load levels. (a) C-6001. (b) C-6002. (c) C-6003

throughout the entire specimen, accompanied by the sound of splitting (Fig. 5(b)). In the C-6003 specimen, macroscopic cracks were observed in the longitudinal direction of the upper end of the specimen, and the bamboo fibers showed buckling failure (Fig. 5(c)). The creep curve measured at the 60% load level is shown in Fig. 6. In general, the three creep specimens under compression performed well due to the satisfactory bonding strength between the bamboo fibers.

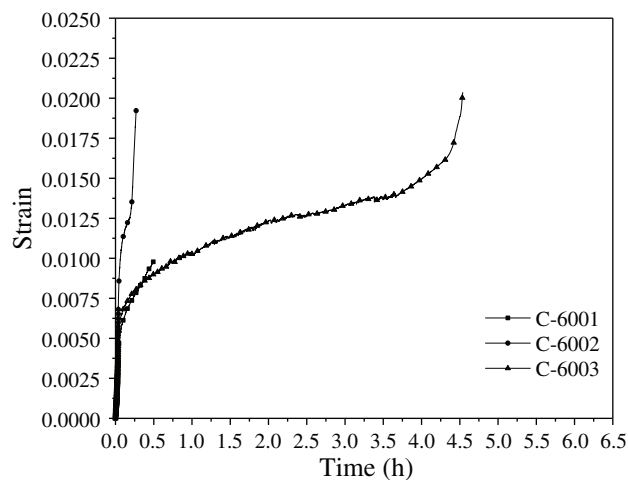


**Figure 6:** Measured creep curves at the 60% load level

Similar to the compressive specimens, no significant visible damage occurred in the tensile creep bamboo specimens at low load levels (below the 40% load level), as shown in Fig. 7. When the short-term tensile stress reached the 60% strength level, the process of tensile fracturing of the fibers can usually be divided into three stages: the formation of micropores, slow crack growth, and rapid crack propagation [58]. The typical failure mode of the recombinant bamboo tensile specimens at high load levels (60% load level) is shown in Fig. 8. As shown in Fig. 9, the T-6001 specimen was subjected to mixed failure (plastic failure and brittle failure) 57 minutes into the test, and macroscopic cracks were observed in its middle part. With increasing time, accompanied by slight fiber breakage, the cracks spread



**Figure 7:** Appearance of the bamboo tensile creep specimens

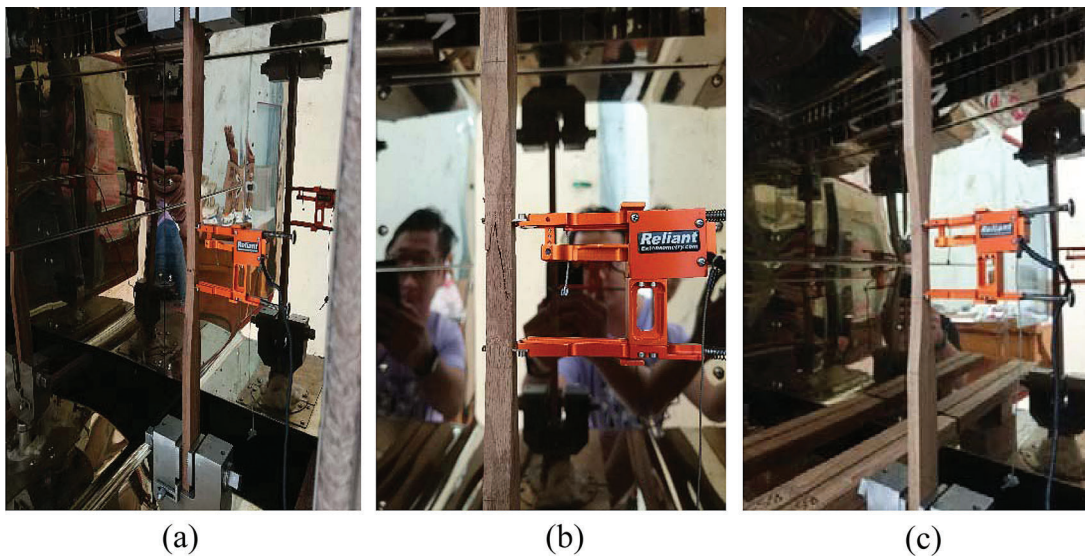


**Figure 8:** Failure phenomena of the bamboo tensile creep specimens at high load levels. (a) T-6001. (b) T-6002. (c) T-6003

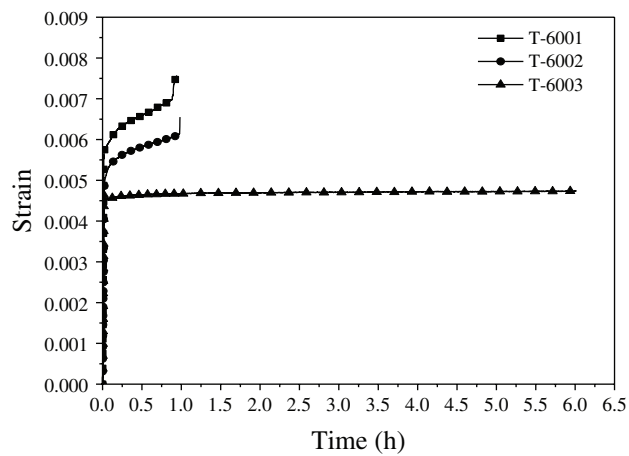


**Figure 9:** Measured creep curves at the 60% load level

randomly and steadily, and mixed damage occurred in the T-6001 specimen. In the process of failure, continuous breakage and plastic deformation of the bamboo fiber occurred, and brittle rupturing occurred suddenly. The T-6002 specimen was subjected to brittle fracturing 62 minutes into the test. When failure occurred due to creep development, the crack spread rapidly, and brittle fracturing suddenly occurred in the middle part of the specimen, accompanied by a cracking sound. At this time, the accumulated energy inside the fibers was completely released. The T-6003 specimen exhibited no distinct signs of macroscopic failure after 6 hours of compressive creep testing.

### 3.2 Creep Test Results and Analysis

#### 3.2.1 Creep Model

When the creep properties of wood materials were investigated, researchers found that the Maxwell model, Kelvin-Voigt model and standard linear solid model each have limitations in terms of reproducing the theoretical model, and the Burgers model can better describe the creep properties of wood materials [59]. The creep deformation of the recombinant bamboo in this study was examined in reference to the creep of wood materials, and the strain-time curves of the compressive creep test data were compared to the theoretical model (Burgers model) and the classical empirical model (Findley model) results.

#### Burgers Model

The Burgers model is a four-element model obtained by connecting the Maxwell model and the Kelvin-Voigt model. As shown in Fig. 10, the Burgers model has the advantages of both the Maxwell model and the Kelvin-Voigt model, which can suitably describe the creep properties of viscoelastic materials and is widely used in the study of viscoelastic materials.

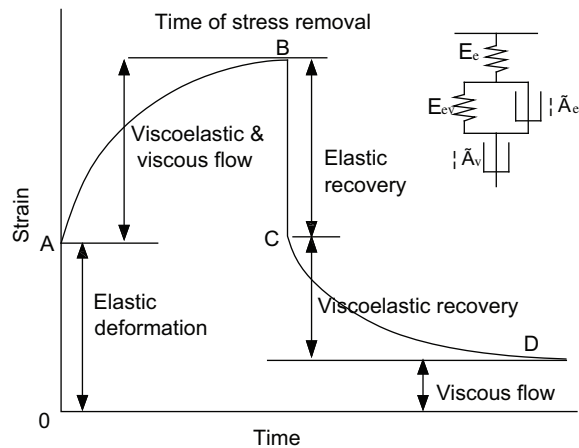


**Figure 10:** The creep curve of the Burgers model

The strain in the Burgers model is composed of elastic deformation, viscous deformation and viscoelastic deformation. To define the constant stress  $\sigma = \sigma_0$ , the constitutive equation of the Burgers model is as follows:

$$\varepsilon(t) = \frac{\sigma_0}{E_e} + \frac{\sigma_0}{\eta_v} t + \frac{\sigma_0}{E_{ev}} \left[ 1 - \exp\left(-\frac{E_{ev}}{\eta_{ev}} t\right) \right] \quad (1)$$

where  $\varepsilon(t)$  is the material strain;  $\sigma_0$  is the constant stress on the material;  $t$  is the load lasting time;  $E_e$  is the instantaneous elastic modulus;  $E_{ev}$  is the delayed elastic modulus;  $\eta_v$  is the viscosity coefficient; and  $\eta_{ev}$  is the viscoelastic coefficient.

To clearly model the creep test results in this study, Eq. (1) is simplified into a parametric form as follows:

$$\varepsilon(t) = A + Bt + C[1 - \exp(-Dt)] \quad (2)$$

where  $\varepsilon(t)$  is the deformation of the material;  $t$  is the load lasting time during creep;  $A$  is the instantaneous elastic strain;  $B$  is the coefficient related to viscous deformation; and  $C$  and  $D$  are the coefficients related to viscoelastic deformation.

#### *Findley Model*

The Findley model is a parabolic empirical model and is generally used to describe the creep behavior of polymer materials. Its model expression is as follows:

$$\varepsilon(t) = y_0 + mt^n \quad (3)$$

where  $\varepsilon(t)$  is the deformation of the material;  $y_0$  is the initial elastic deformation;  $t$  is the load lasting time during creep; and  $m$  and  $n$  are constants that are a function of the test conditions.

#### *3.2.2 Measured and Fitted Creep Curves*

The measured strain-time curves of the compressive creep tests and tensile creep tests are shown in Figs. 11 and 12, respectively. regarding the development of creep deformation, in general, within the first 1.5 hours, creep deformation develops rapidly, and after 1.5 hours, creep deformation tends to develop stably when the stress is lower than the 40% strength level. For the bamboo specimens at high load levels (the 60% load level; C-60 01-03 and T-60 01-03), creep deformation quickly tends to develop nonuniformly and increases rapidly until failure. The fitting curves using the theoretical model (Burgers model) and the classical empirical model (Findley model) are also depicted in these figures. The specimens that fail early in the tests show different creep behaviors compared to the other specimens; thus, these two groups of specimens exhibiting early fracture failure at high load levels (C-60 01-03 and T-60 01-03) were excluded in the fitting process. The fitting curves using the Burgers model and Findley model agree well with the measured curves in terms of the overall trends.

The relevant fitting parameters of compressive creep and tensile creep from both the Burgers model and the Findley model are listed in Tabs. 2 and 3, respectively. The relevant parameters of the theoretical model and empirical model include the instantaneous elastic strain ( $A$ ), coefficient related to the viscous deformation ( $B$ ), coefficients related to the viscoelastic deformation ( $C$  and  $D$ ), correction determinant coefficient ( $R_{2adj}$ ) and coefficients related to the empirical model. In this study, tensile and compressive deformation data are collected by extensometers (Figs. 3(a) and 3(b)). The correlation coefficients ( $R_{2adj}$ ) of the creep deformation data fitted by the two models are above 0.95, which indicates that both the theoretical and empirical models can describe the creep properties of the recombinant bamboo very well. To accurately illustrate the variation in the creep components of the recombinant bamboo, the theoretical model (Burgers model) was used to analyze the short-term creep behaviors of the recombinant bamboo (Section 3.2.3 and Section 3.2.4) and to establish a long-term creep prediction model (Section 4).

#### *3.2.3 Influence of the Load Level on the Creep Performance*

Figure 13 displays the average creep deformation curves of the specimens at the different load levels and the Burgers model fitting curves of the average creep deformation curves. As shown in Fig. 13 and Tabs. 4 and 5, for compressive creep, the results indicate that when the load level increased from 10% to 20%, the total strain ( $\varepsilon_t$ ) of the specimen increased from  $0.660 \times 10^{-3}$  to  $1.462 \times 10^{-3}$ , an increase of 2.22 times; when the load level increased from 20% to 40%, the total strain of the specimen increased from  $1.462 \times 10^{-3}$  to  $4.660 \times 10^{-3}$ , an increase of 3.19 times. For tensile creep, the specific results show that when the load level increased from 10% to 20%, the total strain of the specimens increased from  $1.181 \times 10^{-3}$  to 2.116

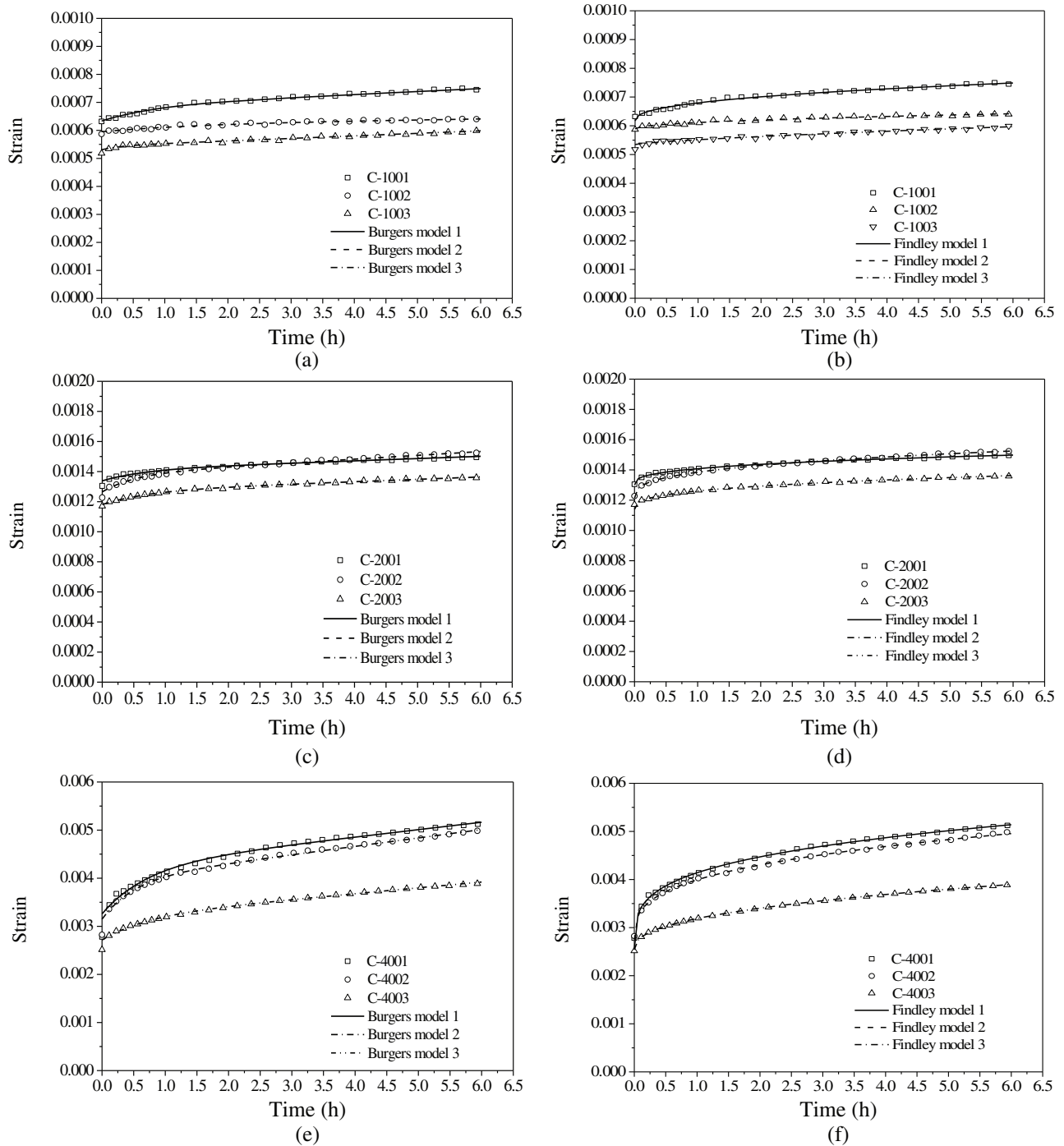


**Figure 11:** Fitted curves and measured curves of compressive creep. (a) Burgers model fitting curves at the 10% load level. (b) Findley model fitting curves at the 10% load level. (c) Burgers model fitting curves at the 20% load level. (d) Findley model fitting curves at the 20% load level. (e) Burgers model fitting curves at the 40% load level. (f) Findley model fitting curves at the 40% load level

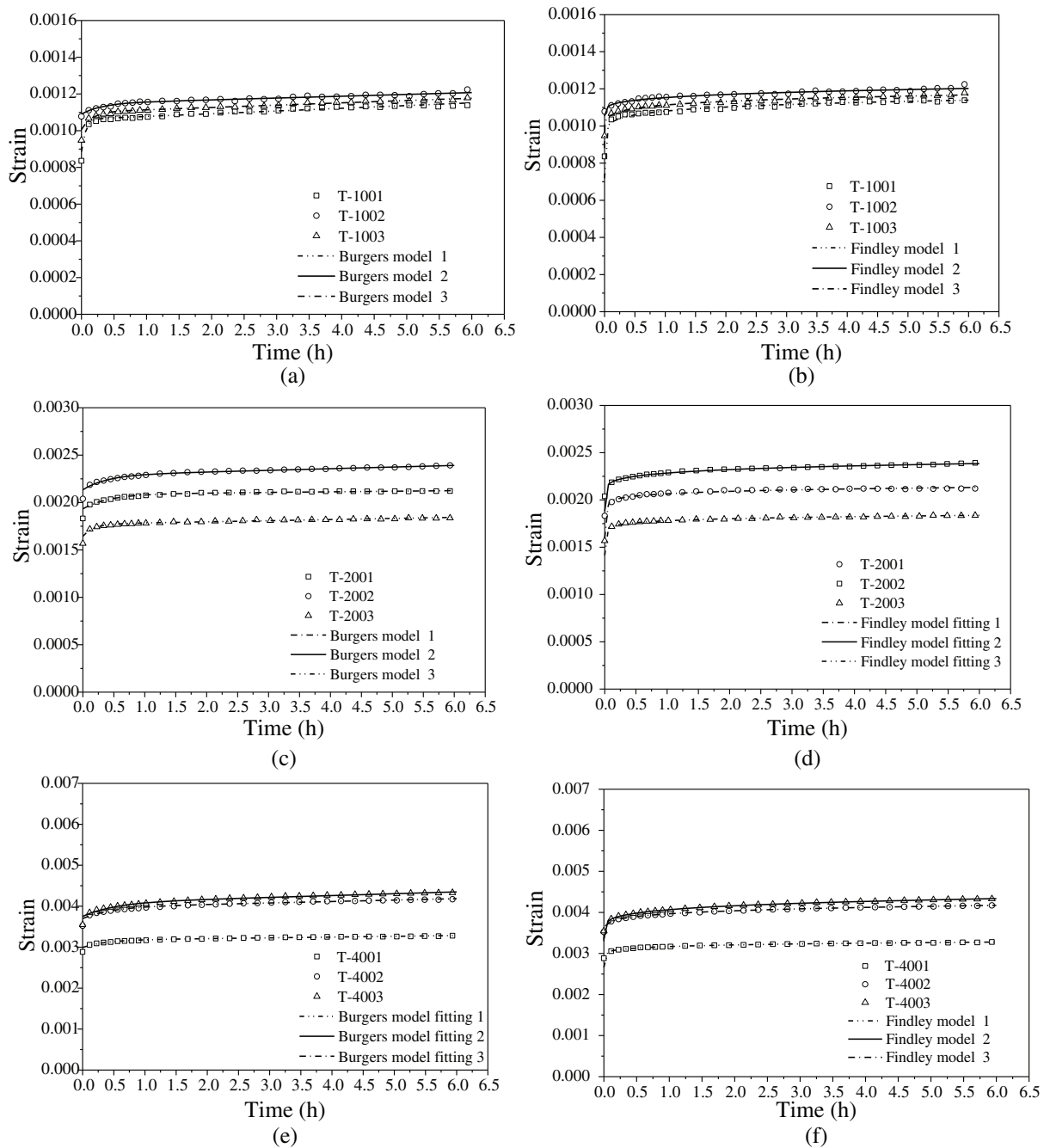


**Figure 12:** Fitted curves and measured curves of tensile creep. (a) Burgers model fitting curves at the 10% load level. (b) Findley model fitting curves at the 10% load level. (c) Burgers model fitting curves at the 20% load level. (d) Findley model fitting curves at the 20% load level. (e) Burgers model fitting curves at the 40% load level. (f) Findley model fitting curves at the 40% load level

$\times 10^{-3}$ , an increase of 1.80 times; when the load level increased from 20% to 40%, the total strain of the specimens increased from  $2.116 \times 10^{-3}$  to  $4.721 \times 10^{-3}$ , an increase of 2.23 times, indicating that the total deformation of creep increased with the increase in load level. Both the compressive and tensile creep increase with increasing load level, and the creep rate increases with increasing load level.

**Table 2:** Fitting parameters of compressive creep

Specimens	Burgers model					Findley model			
	$A \times 10^{-3}$	$B \times 10^{-5}$	$C \times 10^{-5}$	D	$R_{2adj}$	$m \times 10^{-4}$	n	$y_0 \times 10^{-5}$	$R_{2adj}$
C-1001	0.633	1.053	5.283	1.212	0.990	0.626	0.415	0.260	0.987
C-1002	0.595	0.310	2.769	0.604	0.961	0.219	0.489	0.107	0.957
C-1003	0.531	0.905	1.332	3.407	0.972	0.167	0.734	0.123	0.967
Average	0.586	0.756	3.128	1.741	–	0.337	0.546	0.184	–
C-2001	1.340	1.504	7.301	1.502	0.992	1.073	0.339	0.364	0.997
C-2002	1.270	2.548	11.520	1.956	0.997	1.713	0.334	0.573	0.998
C-2003	1.180	1.562	8.963	1.332	0.996	1.219	0.340	0.414	0.996
Average	1.263	1.871	9.261	1.597	–	1.335	0.338	0.451	–
C-4001	3.260	15.301	98.756	1.405	0.992	15.900	0.272	4.317	0.998
C-4002	3.150	17.494	81.512	2.005	0.997	12.400	0.319	3.961	0.999
C-4003	2.720	12.047	48.222	1.398	0.998	6.478	0.413	2.673	0.999
Average	3.043	14.947	76.163	1.603	–	11.593	0.335	3.878	–

**Table 3:** Fitting parameters of tensile creep

Specimens	Burgers model					Findley model			
	$A \times 10^{-3}$	$B \times 10^{-5}$	$C \times 10^{-5}$	D	$R_{2adj}$	$m \times 10^{-4}$	n	$y_0 \times 10^{-5}$	$R_{2adj}$
T-1001	0.886	1.481	1.768	15.624	0.960	3.618	0.084	0.718	0.958
T-1002	1.090	0.995	0.578	3.346	0.971	0.988	0.226	1.050	0.958
T-1003	1.01	1.262	0.949	6.275	0.973	2.316	0.118	8.812	0.978
Average	0.995	1.246	1.098	8.415	–	2.307	0.142	3.526	–
T-2001	1.930	0.631	1.538	2.376	0.980	4.709	0.075	1.590	0.955
T-2002	2.130	1.731	1.534	2.599	0.989	4.055	0.123	1.880	0.994
T-2003	1.640	1.181	1.296	5.925	0.972	3.662	0.081	1.410	0.973
Average	1.900	1.181	1.456	3.633	–	4.142	0.093	1.627	–
T-4001	2.990	1.890	1.787	2.768	0.982	5.072	0.109	2.660	0.994
T-4002	3.700	3.490	2.766	2.178	0.986	6.690	0.149	3.300	0.998
T-4003	3.750	4.441	3.307	1.945	0.988	7.213	0.176	3.350	0.999
Average	3.480	3.274	2.620	2.297	–	6.325	0.145	3.103	–

### 3.2.4 Creep Composition Analysis

In viscoelastic mechanics, creep deformation consists of three parts, including the initial elastic deformation, the viscous deformation that cannot be restored after stress unloading, and the viscoelastic deformation that can be partially restored. To investigate the individual proportions of the creep deformation components of recombinant bamboo at the different load levels, the proportions of elastic, viscous and viscoelastic strain of the total deformation were determined and are summarized in [Tabs. 4](#) and [5](#)

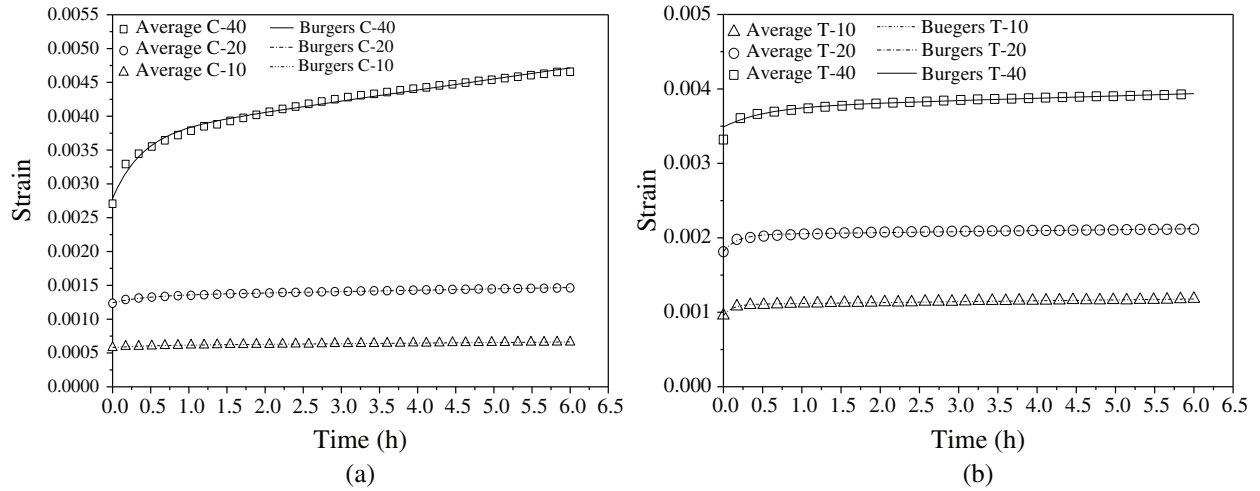


**Figure 13:** Burgers model fitting curves of the average creep deformation. (a) Compressive creep. (b) Tensile creep

**Table 4:** Proportions of the deformation components for compressive creep

Specimens	Strain			Proportions of the deformation components (%)		
	$\varepsilon_0 (\times 10^{-3})$	$\varepsilon_l (\times 10^{-3})$	$\varepsilon_\eta (\times 10^{-4})$	$\varepsilon_0/\varepsilon_l$	$\varepsilon_{ev}/\varepsilon_l$	$\varepsilon_\eta/\varepsilon_l$
C-1001	0.632	0.747	0.610	84.770	7.070	8.150
C-1002	0.587	0.641	0.180	92.860	4.320	2.820
C-1003	0.518	0.596	0.520	89.070	2.240	8.700
Average	0.579	0.661	0.437	88.900	4.540	6.560
C-2001	1.305	1.497	0.840	89.510	4.880	5.610
C-2002	1.227	1.530	1.450	83.010	7.530	9.460
C-2003	1.171	1.360	0.900	86.760	6.590	6.650
Average	1.234	1.462	1.063	86.430	6.330	7.240
C-4001	2.78	5.133	8.850	63.510	19.240	17.250
C-4002	2.824	4.950	9.850	63.640	16.470	19.900
C-4003	2.515	3.896	6.940	69.820	12.380	17.810
Average	2.706	4.660	8.547	65.650	16.030	18.320

according to the test results. The values of the initial elastic deformation ( $\varepsilon_0$ ) and terminal deformation ( $\varepsilon_l$ ) were obtained from the test, and the viscoelastic strain ( $\varepsilon_{ev}$ ) was obtained from the fitted Burgers model (Eq. (2)). According to the monotonicity of the exponential function, 6 hours into the test, the viscoelastic strain ( $\varepsilon_{ev}$ ) is approximately equal to C. Then, the viscous deformation ( $\varepsilon_\eta$ ) is obtained based on Eq. (4), and the viscous deformation ( $\varepsilon_\eta$ ) is calculated via Eq. (1).

$$\varepsilon_\eta = \varepsilon_l - \varepsilon_0 - C \tag{4}$$

**Table 5:** Proportions of the deformation components for tensile creep

Specimens	Strain			Proportions of the deformation components (%)		
	$\epsilon_0 (\times 10^{-3})$	$\epsilon_l (\times 10^{-3})$	$\epsilon_\eta (\times 10^{-4})$	$\epsilon_0/\epsilon_l$	$\epsilon_{ev}/\epsilon_l$	$\epsilon_\eta/\epsilon_l$
T-1001	0.836	1.140	0.770	77.710	15.510	6.780
T-1002	1.078	1.222	0.740	89.200	4.730	6.070
T-1003	0.864	0.945	0.809	91.4288.402	0.012	8.560
Average	0.957	1.181	0.755	86.112	6.751	7.136
T-2001	1.832	2.123	0.390	90.910	7.240	1.850
T-2002	2.039	2.389	1.060	89.160	6.420	4.420
T-2003	1.569	1.835	0.650	89.370	7.060	3.560
Average	1.813	2.116	0.700	89.806	6.906	3.276
T-4001	2.884	3.583	4.140	83.450	4.990	11.560
T-4002	5.017	6.253	1.236	80.233	17.790	1.977
T-4003	3.548	4.329	2.480	86.630	7.640	5.740
Average	3.816	4.721	2.618	83.437	10.140	6.426

The proportions of the elastic, viscoelastic and viscous strain in the total deformation are plotted in Fig. 14. It can be observed that the elastic deformation is relatively large, which dominates the total deformation of the specimens under lasting loading. The viscoelastic deformation and viscous deformation are smaller than the elastic deformation, accounting for a small proportion, indicating that the creep recovery of the recombinant bamboo material is strong and the irreversible residual deformation is relatively small. A low load level has a slight effect on the creep deformation; when the load level increased, the viscoelastic and viscous deformation increased significantly. For compressive creep, when the load level increased from 10% to 20%, the ratio of viscoelastic deformation to total deformation increased from 4.54% to 6.33%, and the ratio of viscous deformation to total deformation increased from

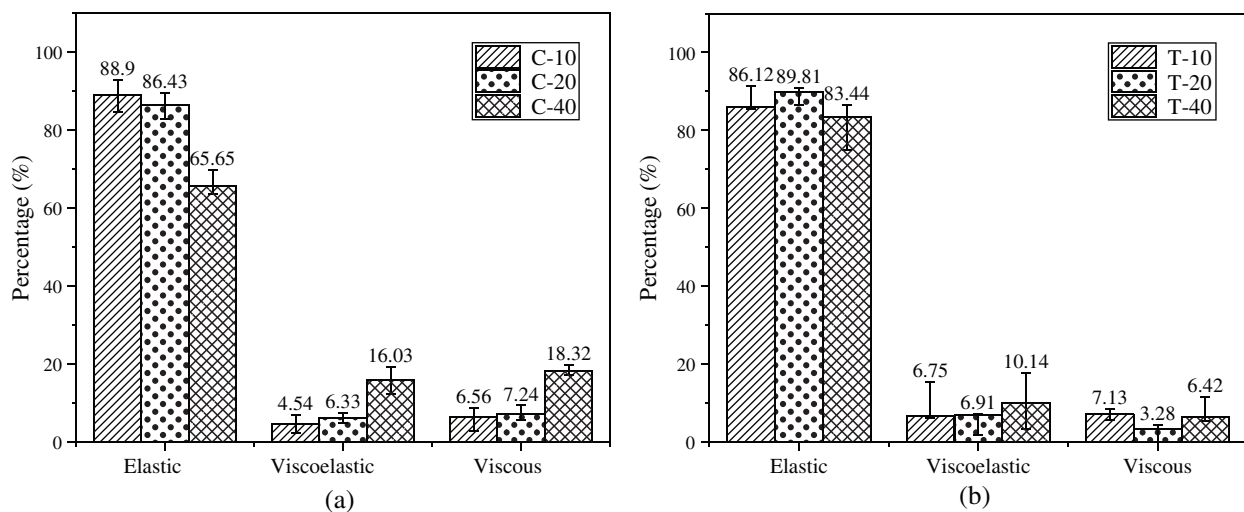


**Figure 14:** Proportions of the creep deformation components. (a) Compressive creep. (b) Tensile creep

6.56% to 7.24%. At the 40% strength load level, the viscoelastic deformation and viscous deformation are 16.03% and 18.32%, respectively. For tensile creep, the percentage of the viscoelastic deformation is between 6.75% and 10.14%, and the percentage of the viscous deformation is between 3.28% and 7.13%. The load level has clear effects on the overall creep deformation and the proportions of creep deformation components for the recombinant bamboo. It can be concluded that the residual deformation of creep will generally increase and the recovery of creep will decrease with increasing load level. According to the analysis of the proportions of the creep deformation components of the recombinant bamboo, the laws reflecting the internal mechanism of the creep deformation were determined, and the long-term creep prediction model was further established.

#### 4 Long-term Creep Prediction Model

To effectively predict the creep behavior of recombinant bamboo, based on the Burgers model (Eq. (2)), the expression for the relative creep coefficient ( $\varepsilon(t)/\bar{\varepsilon}_0$ ) at different load levels is defined as follows:

$$\varepsilon t/\bar{\varepsilon}_0 = \beta_1 + \beta_2 t + \beta_3 [1 - \exp(-\beta_4 t)] \quad (5)$$

where  $\bar{\varepsilon}_0$  is the initial elastic strain at a certain load level;  $t$  is the load lasting time (hours);  $\beta_1 = A/\bar{\varepsilon}_0$ ;  $\beta_2 = B/\bar{\varepsilon}_0$ ;  $\beta_3 = C/\bar{\varepsilon}_0$ ; and  $\beta_4 = E_{ev}/\eta_{ev}$ .

The Burgers model parameters of every group of specimens can be calculated, and parameters  $\beta_1$ ,  $\beta_2$ ,  $\beta_3$  and  $\beta_4$  can be obtained by dividing the corresponding model parameters by  $\bar{\varepsilon}_0$  for a specific load level. Defining parameter  $\gamma$  as the stress ratio, coefficients  $\beta_1$ ,  $\beta_2$ ,  $\beta_3$  and  $\beta_4$  are related to parameter  $\gamma$ , and the creep model taking into account the load level can accordingly be determined based on the test results.

##### 4.1 Predictive Model of Compressive Creep

The average creep deformation curves of the specimens at the different compressive load levels are shown in Fig. 13(a), and the Burgers model fitting curves can be obtained based on these average creep deformation curves for the different load levels. The creep deformation expression at the different compressive load levels can be given as:

10% load level:

$$\varepsilon_{10\%}(t) = 0.586 \times 10^{-3} + 7.56 \times 10^{-6} t + 3.128 \times 10^{-5} [1 - \exp(-1.741t)] \quad (6)$$

20% load level:

$$\varepsilon_{20\%}(t) = 1.263 \times 10^{-3} + 1.871 \times 10^{-5} t + 9.261 \times 10^{-5} [1 - \exp(-1.597t)] \quad (7)$$

40% load level:

$$\varepsilon_{40\%}(t) = 3.043 \times 10^{-3} + 1.4947 \times 10^{-4} t + 7.6163 \times 10^{-4} [1 - \exp(-1.603t)] \quad (8)$$

where  $t$  is the load lasting time (hours).

The parameters for the relative creep coefficient ( $\varepsilon(t)/\bar{\varepsilon}_0$ ) expression can be obtained by dividing the corresponding parameters in Eqs. (6), (7), and (8) by the initial elastic strain  $\bar{\varepsilon}_0$ , as listed in Tab. 6.

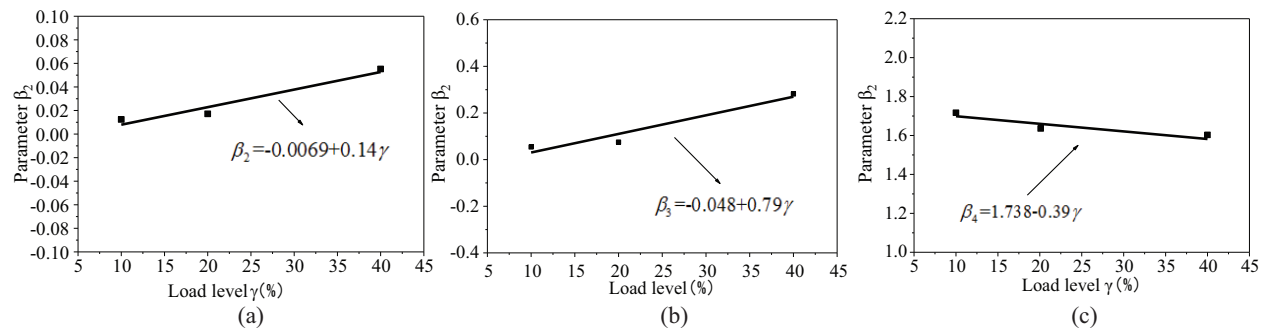
Because  $\beta_1$  is very close to 1.0 at the different load levels, the value of  $\beta_1$  is assumed to be 1.0. The relationship between the model parameters of compressive creep and the load levels are shown in Fig. 15, and  $\beta_2$ ,  $\beta_3$ , and  $\beta_4$  are approximately linear with load level  $\gamma$ . The linear expression between model parameter  $\beta$  (representing  $\beta_2$ ,  $\beta_3$ , and  $\beta_4$ ) and load level  $\gamma$  can be assumed to be:

$$\beta = a + m\gamma \quad (9)$$

where  $\beta$  is the model parameter;  $\gamma$  is the load level; and  $a$  and  $m$  are constants.

**Table 6:** Model parameters of compressive creep at the different load levels

Load levels	Initial elastic strain average	Parameters			
	$\bar{\varepsilon}_0$	$\beta_1$	$\beta_2$	$\beta_3$	$\beta_4$
10%	0.000579	1.012	0.013	0.054	1.741
20%	0.001234	1.023	0.015	0.075	1.597
40%	0.002706	1.124	0.055	0.281	1.603

**Figure 15:** Relationship between the model parameters of compressive creep and load levels. (a)  $\gamma - \beta_2$ . (b)  $\gamma - \beta_3$ . (c)  $\gamma - \beta_4$ 

It can be seen from Fig. 15 that the model parameters  $\beta_2$  and  $\beta_3$  of compressive creep increase linearly with the increase in load level  $\gamma$  and that the model parameter  $\beta_4$  decreases linearly with the increase in load level  $\gamma$ . The expressions of these model parameters can be given as:

$$\begin{aligned}
 \beta_1 &= 1.0 \\
 \beta_2 &= -0.0069 + 0.14\gamma \\
 \beta_3 &= -0.048 + 0.79\gamma \\
 \beta_4 &= 1.738 - 0.39\gamma
 \end{aligned} \tag{10}$$

The expressions of the model parameters (Eq. (10)) were substituted into Eq. (5) to obtain the predictive model of compressive creep for the recombinant bamboo. The expression is as follows:

$$\zeta_\gamma = 1 + (-0.0069 + 0.14\gamma)t + (-0.048 + 0.79\gamma)\{1 - \exp[-(1.738 - 0.39\gamma)t]\} \tag{11}$$

where  $\gamma$  is the load level (%);  $\zeta_\gamma$  is the relative creep coefficient at a certain load level; and  $t$  is the load lasting time during creep (hours).

#### 4.2 Predictive Model of Tensile Creep

The average creep deformation curves of the specimens at the different tensile load levels are shown in Fig. 13(b), following a fitting process similar to that performed for the compressive creep deformation. The Burgers model fitting curves can also be obtained for the tensile creep. The creep deformation expression at the different tensile load levels can be given as:

10% load level:

$$\varepsilon_{10\%}(t) = 0.995 \times 10^{-3} + 1.246 \times 10^{-6}t + 1.098 \times 10^{-4}[1 - \exp(-8.415t)] \tag{12}$$

20% load level:

$$\varepsilon_{20\%}(t) = 1.9 \times 10^{-3} + 1.181 \times 10^{-5}t + 1.456 \times 10^{-4}[1 - \exp(-3.633t)] \quad (13)$$

40% load level:

$$\varepsilon_{40\%}(t) = 3.480 \times 10^{-3} + 3.274 \times 10^{-5}t + 2.620 \times 10^{-4}[1 - \exp(-2.297t)] \quad (14)$$

where  $t$  is the load lasting time (hours).

Similar to the compressive creep model parameters, the parameters for the relative creep coefficient ( $\varepsilon(t)/\bar{\varepsilon}_0$ ) expression for tensile creep can also be obtained by dividing the corresponding parameters in Eqs. (12), (13), and (14) by the initial elastic strain  $\bar{\varepsilon}_0$ , as listed in Tab. 7.

**Table 7:** Model parameters of tensile creep at different load levels

Load levels	Initial strain average $\bar{\varepsilon}_0$	Parameters			
		$\beta_1$	$\beta_2$	$\beta_3$	$\beta_4$
10%	0.000957	1.039	0.013	0.115	8.793
20%	0.001813	1.048	0.007	0.080	3.633
40%	0.003816	0.87867	0.01035901	0.0686635663566352	2.247

The value of  $\beta_1$  is also assumed to be 1.0. The relationship between the model parameters of tensile creep and the load levels are shown in Fig. 16. Model parameters  $\beta_2$ ,  $\beta_3$ , and  $\beta_4$  decrease linearly with the increase in load level  $\gamma$ , and the linear expression between model parameters  $\beta_2$ ,  $\beta_3$ , and  $\beta_4$  and load level  $\gamma$  can be given as:

$$\begin{aligned} \beta_1 &= 1.0 \\ \beta_2 &= 0.0125 - 0.00013\gamma \\ \beta_3 &= 0.1271 - 0.002\gamma \\ \beta_4 &= 10.1235 - 0.2128\gamma \end{aligned} \quad (15)$$

Substituting Eq. (15) into Eq. (5), the predictive model of tensile creep for the recombinant bamboo can be proposed as follows:

$$\zeta_\gamma = 1 + (0.0125 - 0.00013\gamma)t + (0.1271 - 0.002\gamma)\{1 - \exp[-(10.1235 - 0.2128\gamma)t]\} \quad (16)$$

where  $\gamma$  is the load level (%);  $\zeta_\gamma$  is the relative creep coefficient at a certain load level; and  $t$  is the load lasting time during creep (hours).

### 4.3 Validation of the Predictive Model

To demonstrate the validity of the proposed model for the recombinant bamboo, the strain-time curves of the recombinant bamboo as predicted by the proposed model at the different compressive load levels and different tensile load levels are shown in Figs. 17 and 18, respectively. The comparisons show that the proposed model can describe the creep behavior of the recombinant bamboo with increasing time, including the rapid development in the early stage and the stable development in the middle and late stages. At the same time, the proposed model may illustrate the significant effects of the load level. The proposed model is able to accurately evaluate the strain-time behavior of the recombinant bamboo while considering the load level.

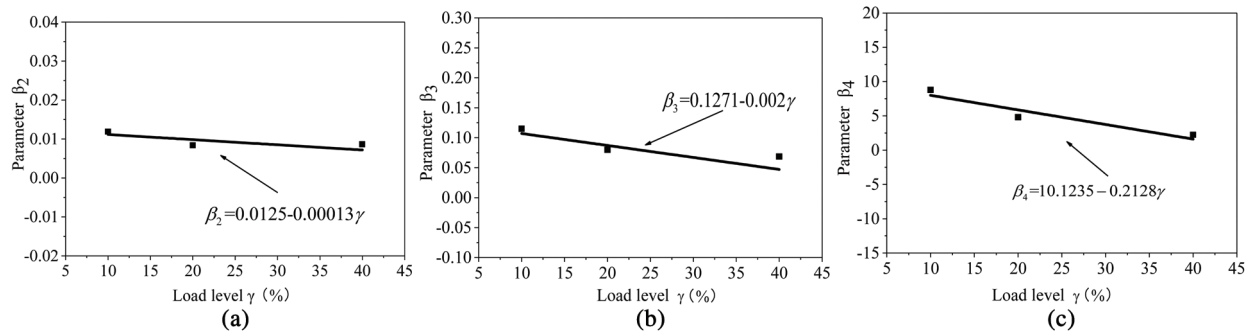


**Figure 16:** Relationship between the model parameters of tensile creep and load levels. (a)  $\gamma - \beta_2$ . (b)  $\gamma - \beta_3$ . (c)  $\gamma - \beta_4$

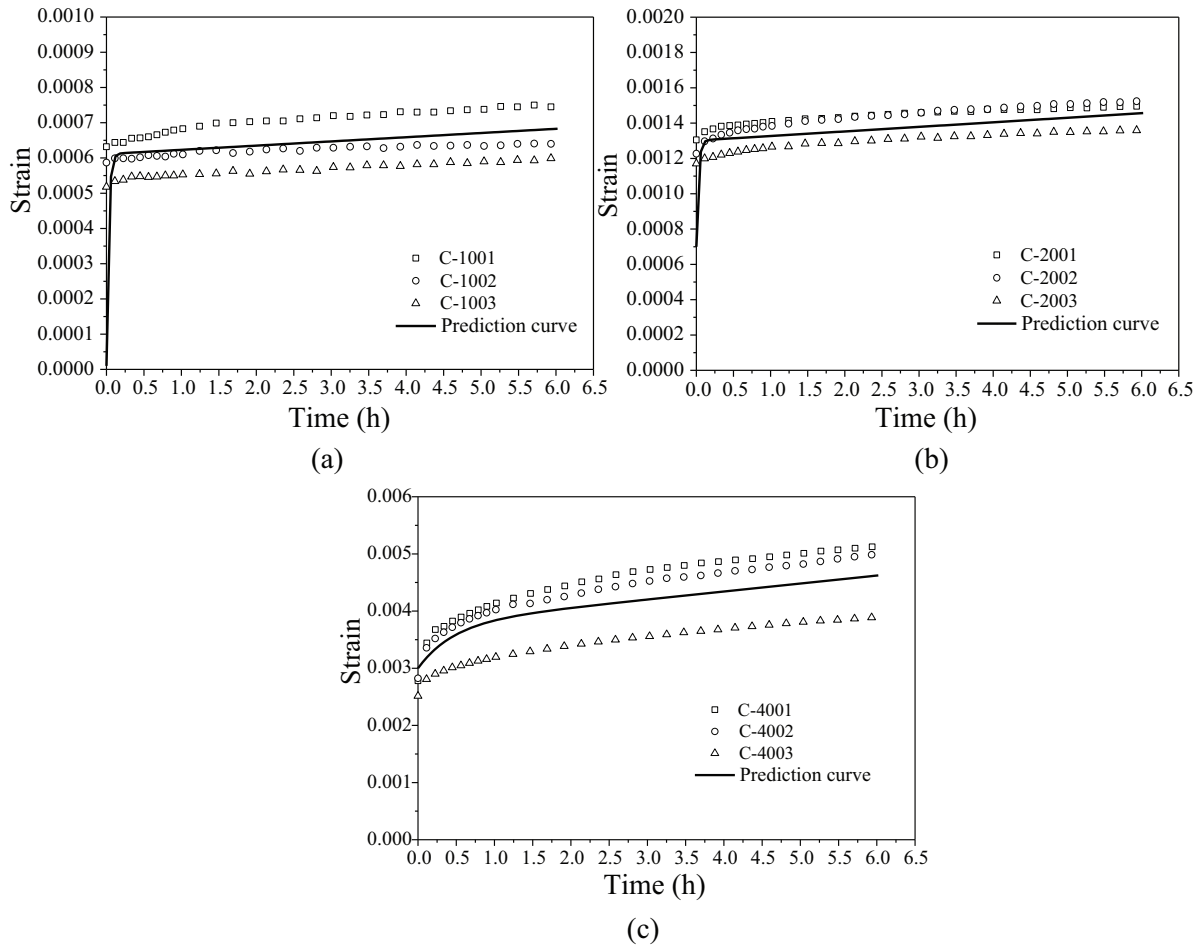


**Figure 17:** Predicted curves of compressive creep for the recombinant bamboo by the proposed model. (a) 10% load level. (b) 20% load level. (c) 40% load level

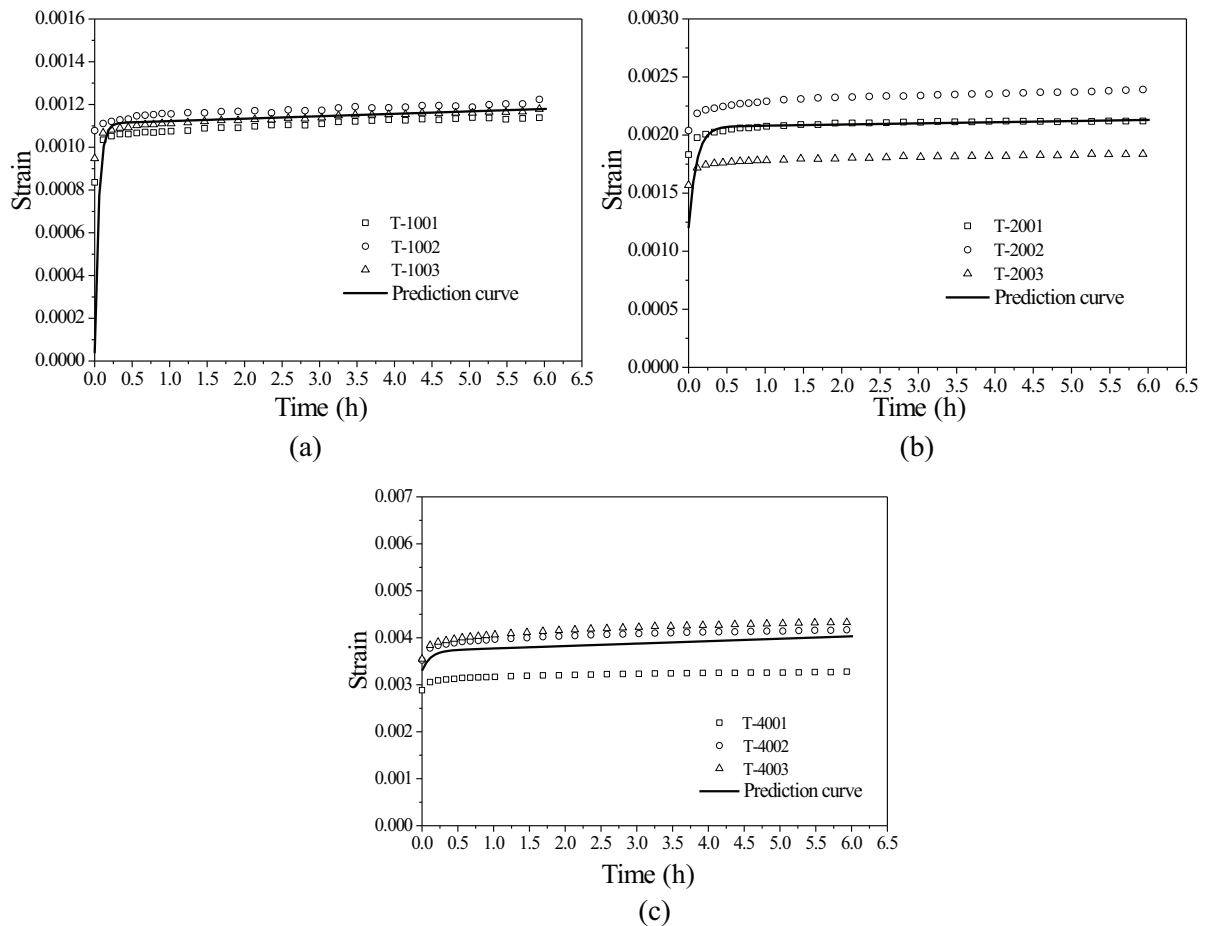


**Figure 18:** Predicted curves of tensile creep for the recombinant bamboo by the proposed model. (a) 10% load level. (b) 20% load level. (c) 40% load level

## 5 Conclusions and Discussion

In this study, based on viscoelastic mechanics theories, aiming at the short-term compressive creep and tensile creep of recombinant bamboo, creep tests of recombinant bamboo at different load levels were carried out. The compressive and tensile creep behaviors of recombinant bamboo under constant-temperature and constant-humidity conditions were examined, and creep prediction models based on the Burgers model were proposed. The conclusions were as follows:

1. The typical failure mode of the recombinant bamboo specimens under a lasting load at a high load level (60% strength level) was buckling failure and brittle fracturing due to compressive creep and tensile creep development, respectively. When the load is lower than the 40% strength level, no clear failure signs can be observed on the surfaces of the specimens.
2. Under certain temperature and humidity conditions, for the bamboo specimens at high load levels (60% strength level), creep deformation initially develops unsteadily and rapidly increases until failure; for the bamboo specimens at low load levels (lower than the 40% strength level), creep deformation develops rapidly in the early stage (within 1.5 hours) and develops stably in the middle and late stages (after 1.5 hours).

3. The total compressive and tensile deformations of the recombinant bamboo increase with the increase in load level. Through analysis of the changes in elastic, viscoelastic and viscous deformation as percentages of the total deformation, it can be seen that the load level has a notable effect on the overall creep deformation and the proportions of creep deformation components. Under the condition of a higher load level, the creep rate is higher, and the development of creep is more notable. The residual deformation of creep will generally increase and the recovery of creep will decrease with increasing load level.
4. Based on the Burgers model, predictive models that can take into account load levels were proposed to evaluate the compressive and tensile creep behaviors of the recombinant bamboo. The comparisons show that the proposed model is able to evaluate the strain-time behavior of recombinant bamboo with good accuracy.

This study mainly considers the effects of load levels on the compressive and tensile creep properties of recombinant bamboo and long-term predictive models under certain conditions of temperature and humidity. However, many factors, such as temperature and humidity, affect the creep of recombinant bamboo; additionally, the coupling of multiple factors has not been discussed. Their effects on the creep behavior of recombinant bamboo will be the focus of the next phase of research.

**Funding Statement:** This work was supported by the National Natural Science Foundation of China (No. 51208262 and No. 51778300), the Natural Science Foundation of Jiangsu Province (No. BK20191390), the 333 Project (No. BRA2016421) and the Qinglan Project of Jiangsu Province (QL2017).

**Conflicts of Interest:** The authors declare that they have no conflicts of interest to report regarding the present study.

## References

1. Ding, L. N., Liu, X., Wang, X., Huang, H., Wu, Z. (2018). Mechanical properties of pultruded basalt fiber-reinforced polymer tube under axial tension and compression. *Construction and Building Materials*, 176, 629–637. DOI 10.1016/j.conbuildmat.2018.05.036.
2. Wang, L. B., Wu, Y., Noori, M. (2015). Parameters of static response of carbon fiber reinforced polymer (CFRP) suspension cables. *Journal of Central South University*, 22(8), 3123–3132. DOI 10.1007/s11771-015-2849-3.
3. Ding, L. N., Liu, N., Liu, Y., Liu, J. X., Wang, X. (2019). Correlation analysis of tensile strength and chemical composition of basalt fiber roving. *Polymer Composites*, 40(7), 2959–2966. DOI 10.1002/pc.25138.
4. Zhang, Y. X. (2013). Analytical method on RC member strengthened by strain hardening cementitious composite in flexural failure. *Journal of Building Structures*, 34(12), 121–127.
5. Zhang, Y. X., Peng, H., Lv, W. (2017). Shear stress transfer model for evaluating the fracture behaviour of SHCCS for RC shear strengthening. *Magazine of Concrete Research*, 70(10), 1–7.
6. Khalil, H. P., Bhat, I. U., Jawaid, M., Zaidon, A., Hermawan, D. et al. (2012). Bamboo fibre reinforced biocomposites: a review. *Materials and Design*, 42, 353–368. DOI 10.1016/j.matdes.2012.06.015.
7. Rao, K. M. M., Rao, K. M. (2007). Extraction and tensile properties of natural fibers: vakka, date and bamboo. *Composite Structures*, 77(3), 288–295. DOI 10.1016/j.compstruct.2005.07.023.
8. Yang, F., Hai, F., Dai, F. (2007). Study on the properties of the recombinant bamboo by finite element method. *Composites Part B*, 115, 151–159.
9. Lakkad, S., Patel, J. (1981). Mechanical-properties of bamboo, a natural composite. *Fibre Science and Technology*, 14(4), 319–322. DOI 10.1016/0015-0568(81)90023-3.
10. Tian, L. M., Kou, Y., Hao, J. (2019). Axial compressive behaviour of sprayed composite mortar-original bamboo composite columns. *Construction and Building Materials*, 215, 726–736. DOI 10.1016/j.conbuildmat.2019.04.234.
11. Li, H., Wang, B. J., Wei, P. X. (2019). Cross-laminated timber (CLT) in China: a state-of-the-art. *Journal of Bioresources and Bioproducts*, 4(1), 22–30.

12. Tian, L. M., Kou, Y. F., Hao, J. P. (2019). Flexural behavior of sprayed lightweight composite mortar-original bamboo composite beams: experimental study. *BioResources*, 14(1), 500–517.
13. Nurdiah, E. A. (2016). The potential of bamboo as building material in organic shaped buildings. *Procedia - Social and Behavioral Sciences*, 216, 30–38. DOI 10.1016/j.sbspro.2015.12.004.
14. Chung, K. F., Yu, W. K. (2002). Mechanical properties of structural bamboo for bamboo scaffoldings. *Engineering Structures*, 24(4), 429–442. DOI 10.1016/S0141-0296(01)00110-9.
15. Flander, K. D., Rovers, R. (2009). One laminated bamboo-frame house per hectare per year. *Construction and Building Materials*, 23(1), 210–218. DOI 10.1016/j.conbuildmat.2008.01.004.
16. Sharma, B., Gato, A., Bock, M., Ramage, M. H. (2015). Engineered bamboo for structural applications. *Construction and Building Materials*, 81, 66–73. DOI 10.1016/j.conbuildmat.2015.01.077.
17. Wang, Z., Dong, W., Zhou, J., Gong, M. (2018). Effect of macro characteristics on rolling shear properties of fast-growing poplar wood laminations. *Wood Research*, 63(2), 227–238.
18. Chen, G., Li, H. T., Zhou, T., Li, C. L. (2015). Experimental evaluation on mechanical performance of OSB webbed parallel strand bamboo I-joist with holes in the web. *Construction and Building Materials*, 101, 91–98. DOI 10.1016/j.conbuildmat.2015.10.041.
19. Tian, L. M., Kou, Y., Hao, J. (2017). Study on flexural behavior of bamboo composite slabs with sprayed thermal insulation material. *Journal of Huazhong University of Science and Technology*, 45(11), 41–45.
20. Lv, Q. F., Ding, Y., Liu, Y. (2019). Study of the bond behaviour between basalt fibre-reinforced polymer bar/sheet and bamboo engineering materials. *Advances in Structural Engineering*, 22(14), 3121–3133. DOI 10.1177/1369433219858725.
21. Wei, Y., Wang, X. W., Li, G. F. (2014). Mechanical properties test of bamboo scrimber flexural specimens reinforced with bars. *Acta Materiae Compositae Sinica*, 31(4), 1030–1036.
22. Wang, Z., Zhou, J., Dong, W., Yao, Y., Gong, M. (2018). Influence of technical characteristics on the rolling shear properties of cross laminated timber by modified planar shear tests. *Maderas Ciencia Y Tecnologia*, 20(3), 469–478.
23. Chen, G., He, B. (2017). Stress-strain constitutive relation of OSB under axial loading: an experimental investigation. *Bioresources*, 12(3), 6142–6156.
24. Wang, Z. Q., Zhou, J. H., Meng, G., Ying, H. C. (2016). Evaluation of modulus of elasticity of laminated strand lumber by non-destructive evaluation technique. *Bioresources*, 11(1), 626–633.
25. Obataya, E., Kitin, P., Yamauchi, H. (2007). Bending characteristics of bamboo (*Phyllostachys pubescens*) with respect to its fiber-foam composite structure. *Wood Science and Technology*, 41(5), 385–400. DOI 10.1007/s00226-007-0127-8.
26. Jain, S., Kumar, R. K., Jindal, U. C. (1992). Mechanical behaviour of bamboo and bamboo composite. *Journal of Materials Science*, 27(17), 4598–4604. DOI 10.1007/BF01165993.
27. Li, H. T., Wu, G., Zhang, Q., Deeks, A., Su, J. (2018). Ultimate bending capacity evaluation of laminated bamboo lumber beams. *Construction and Building Materials*, 160, 365–375. DOI 10.1016/j.conbuildmat.2017.11.058.
28. Lo, T. Y., Cui, H., Tang, P. W., Leung, H. C. (2008). Strength analysis of bamboo by microscopic investigation of bamboo fibre. *Construction and Building Materials*, 22(7), 1532–1535. DOI 10.1016/j.conbuildmat.2007.03.031.
29. Zou, Z., Wu, J., Zhang, X. (2019). Influence of moisture content on mechanical properties of bamboo scrimber. *Journal of Materials in Civil Engineering*, 31(7), 06019004. DOI 10.1061/(ASCE)MT.1943-5533.0002746.
30. Kumar, A., Vlach, T., Laiblova, L., Hrouda, M., Kasal, B. et al. (2016). Engineered bamboo scrimber: influence of density on the mechanical and water absorption properties. *Construction and Building Materials*, 127, 815–827. DOI 10.1016/j.conbuildmat.2016.10.069.
31. Das, M., Pal, A., Chakraborty, D. (2006). Effects of mercerization of bamboo strips on mechanical properties of unidirectional bamboo-novolac composites. *Journal of Applied Polymer Science*, 100(1), 238–244. DOI 10.1002/app.23028.
32. Hu, D., Song, B., Dang, L., Zhang, Z. (2018). Effect of strain rate on mechanical properties of the bamboo material under quasi-static and dynamic loading condition. *Composite Structures*, 200, 635–646. DOI 10.1016/j.compstruct.2018.05.107.

33. Okubo, K., Fujii, T., Yamamoto, Y. (2004). Development of bamboo-based polymer composites and their mechanical properties. *Composites Part A-applied Science and Manufacturing*, 35(3), 377–383. DOI 10.1016/j.compositesa.2003.09.017.
34. Ozyhar, T., Hering, S., Niemz, P. (2012). Moisture-dependent elastic and strength anisotropy of European beech wood in tension. *Journal of Materials Science*, 47(16), 6141–6150. DOI 10.1007/s10853-012-6534-8.
35. Ozyhar, T., Hering, S., Sanabria, S. J., Niemz, P. (2012). Determining moisture-dependent elastic characteristics of beech wood by means of ultrasonic waves. *Wood Science & Technology*, 47(2), 329–341. DOI 10.1007/s00226-012-0499-2.
36. Ozyhar, T., Hering, S., Niemz, P. (2013). Moisture-dependent orthotropic tension-compression asymmetry of wood. *Holzforschung*, 67(4), 395–404. DOI 10.1515/hf-2012-0089.
37. Huang, Z., Sun, Y., Musso, F. (2017). Assessment of bamboo application in building envelope by comparison with reference timber. *Construction and Building Materials*, 156, 844–860. DOI 10.1016/j.conbuildmat.2017.09.026.
38. Der Lugt, P. V., Den Dobbelsesteen, A. A., Janssen, J. J. (2006). An environmental, economic and practical assessment of bamboo as a building material for supporting structures. *Construction and Building Materials*, 20(9), 648–656. DOI 10.1016/j.conbuildmat.2005.02.023.
39. Gottron, J., Harries, K. A., Xu, Q. (2014). Creep behaviour of bamboo. *Construction and Building Materials*, 66, 79–88. DOI 10.1016/j.conbuildmat.2014.05.024.
40. Zong, G. G., Hao, X. L., Hao, J. X. (2020). High-strength, lightweight, co-extruded wood flour-polyvinyl chloride/lumber composites: effects of wood content in shell layer on mechanical properties, creep resistance, and dimensional stability. *Journal of Cleaner Production*, 244, 118860.
41. Hao, X. L., Xin, Y., Sun, L. C. (2019). Mechanical properties, creep resistance, and dimensional stability of core/shell structured wood flour/polyethylene composites with highly filled core layer. *Construction and Building Materials*, 226(11), 879–887. DOI 10.1016/j.conbuildmat.2019.07.329.
42. Navi, P., Pittet, V., Plummer, C. J. G. (2002). Transient moisture effects on wood creep. *Wood Science and Technology*, 36(6), 447–462.
43. Hoseinzadeh, F., Zabihzadeh, S. M., Dastoorian, F. (2019). Creep behavior of heat treated beech wood and the relation to its chemical structure. *Construction and Building Materials*, 226(11), 220–226. DOI 10.1016/j.conbuildmat.2019.07.181.
44. Pulngern, T., Chitsamran, T., Chucheeesakul, S. (2016). Effect of temperature on mechanical properties and creep responses for wood/PVC composites. *Construction and Building Materials*, 111(5), 191–198. DOI 10.1016/j.conbuildmat.2016.02.051.
45. Angellier, N., Dubois, F., Pitti, R. M. (2017). Influence of hygrothermal effects in the fracture process in wood under creep loading. *Engineering Fracture Mechanics*, 177(5), 153–166. DOI 10.1016/j.engfracmech.2017.04.009.
46. Tamrakar, S., Lopez-Anido, R. A., Kiziltas, A. (2011). Time and temperature dependent response of a wood-polypropylene composite. *Composites Part A: Applied Science and Manufacturing*, 42(7), 834–842. DOI 10.1016/j.compositesa.2011.03.011.
47. Reichel, S., Kaliske, M. (2015). Hygro-mechanically coupled modelling of creep in wooden structures, part II: influence of moisture content. *International Journal of Solids and Structures*, 77(12), 45–64. DOI 10.1016/j.ijsolstr.2015.07.029.
48. Ozyhar, T., Hering, S., Niemz, P. (2013). Viscoelastic characterization of wood: time dependence of the orthotropic compliance in tension and compression. *Journal of Rheology*, 57(2), 699–717. DOI 10.1122/1.4790170.
49. Wang, J. B., Lam, F., Foschi, R. O. (2012). Duration-of-load and creep effects in strand-based wood composite: a creep-rupture model. *Wood Science and Technology*, 46(1), 375–391. DOI 10.1007/s00226-011-0401-7.
50. Gottron, J., Harries, K. A., Xu, Q. (2014). Creep behaviour of bamboo. *Construction and Building Materials*, 66, 79–88. DOI 10.1016/j.conbuildmat.2014.05.024.
51. Xu, Y., Lee, S., Wu, Q. (2011). Creep analysis of bamboo high-density polyethylene composites: effect of interfacial treatment and fiber loading level. *Polymer Composites*, 32(5), 692–699. DOI 10.1002/pc.21088.

52. Kanzawa, E., Aoyagi, S., Nakano, T. (2011). Vascular bundle shape in cross-section and relaxation properties of Moso bamboo (*Phyllostachys pubescens*). *Materials Science and Engineering, C*, 31(5), 1050–1054. DOI 10.1016/j.msec.2011.03.004.
53. Ma, X., Shi, S. Q., Wang, G., Fei, B., Jiang, Z. (2018). Long creep-recovery behavior of bamboo-based products. *Journal of Wood Science*, 64(2), 119–125. DOI 10.1007/s10086-017-1683-7.
54. ASTM D 143-14. (2000). *Standard test methods for small clear specimens of timber*. ASTM Committee, West Conshohocken PA, USA.
55. GB/T 1928-2009. (2009). *Test method for physical and mechanical properties of wood*. China Standards Press, Beijing, China.
56. GB/T 1935-2009. (2009). *Method of testing in compressive strength parallel to grain of wood*. China Standards Press, Beijing, China.
57. GB/T 1938-2009. (2009). *Method of testing in tensile strength parallel to grain of wood*. China Standards Press, Beijing, China.
58. Li, F. T., Cheng, Z. D., Zhang, Y. (1980). Fracture process and mechanism of fibers. *Journal of Donghua University (Natural Science Edition)*, 3, 109–124.
59. Wang, F. H. (2005). *Rheology of Wood Materials*. Nanjing: Northeast Forestry University Education Press, 15–17.